Mechanism Responsible for the Complete Suppression of Kármán Vortex in Flows Past a Wavy Square-Section Cylinder

2010 Chinese Phys. Lett. 27 034702

(http://iopscience.iop.org/0256-307X/27/3/034702)

CHIN. PHYS. LETT. Vol. 27, No. 3 (2010) 034702

Mechanism Responsible for the Complete Suppression of Kármán Vortex in Flows Past a Wavy Square-Section Cylinder *

LIN Li-Ming(林黎明)[1**], LING Guo-Can(凌国灿)[2], WU Ying-Xiang(吴应湘)[1]

[1] *The Division of Engineering Sciences, Institute of Mechanics, Chinese Academy of Sciences, Beijing 100190*
[2] *The Stake Key Laboratory of Nonlinear Mechanics, Institute of Mechanics, Chinese Academy of Sciences, Beijing 100190*

(Received 15 August 2009)

The Kármán vortex shedding is totally suppressed in flows past a wavy square-section cylinder at a Reynolds number of 100 and the wave steepness of 0.025. Such a phenomenon is illuminated by the numerical simulations. In the present study, the mechanism responsible for it is mainly attributed to the vertical vorticity. The geometric disturbance on the rear surface leads to the appearance of spanwise flow near the base. The specific vertical vorticity is generated on the rear surface and convecting into the near wake. The wake flow is recirculated with the appearance of the pair of recirculating cells. The interaction between the upper and lower shear layers is weakened by such cells, so that the vortex rolls could not be formed and the near wake flow becomes stable.

PACS: 47. 32. C−, 47. 15. Tr DOI: 10.1088/0256-307X/27/3/034702

It has been known for a long time that the vortex shedding can be suppressed in the wake of bluff bodies by normal two-dimensional methods, like adding splitter plates.[1,2] In recent decades, the three-dimensional geometric disturbance has been proposed to control the vortex dynamics in the near wake with the aim of interfering and weakening regular vortex shedding. For example, the flat plate (normal to inflow) with the wavy stagnation surfaces and the wavy-leading-edge rectangular cylinder at a Reynolds number of 40000 lead to the complete suppression of vortex shedding.[3] Similar result is also obtained in recent numerical simulations for flows past a wavy square-section cylinder at a Reynolds number of 100 with the wave steepness about $0.025 \sim 0.03$,[4,5] which is defined by the ratio of the wave height W to the wavelength λ. When the wave steepness increases or decreases, such as 0.167 or 0.006, such a phenomenon is associated with the unsteady wake flow.[6] Meanwhile, the mean drag reductions reach up to about 30%,[3] 16%[4] and 13%.[5] This indicates that the introduction of such disturbance could be applied in the structural device as a beneficial effect, such as reducing the fluid force on bluff bodies, as well as the flow-induced vibration.

Recently in the study of flow around the wavy square-section cylinder, Darekar and Sherwin[4] attributed the vortex suppression to the appearance of additional vorticity (streamwise and vertical components), particularly the streamwise component. This further leads to the distortion of two-dimensional spanwise vorticity and shear layers downstream, based on the specific distribution of streamwise vorticity near the lateral side of cylinder, rather than in the near wake. However, as pointed out by Ling and Lin,[5] there are some critical errors in their derived transformed N-S equations and the extra terms due to the transformation. Thus their above numerical results are still questionable. Understanding of the suppression of Kármán vortex is still far from the completeness. The main motivation is put in illuminating such physical mechanism with the correct governing equations, based on detailed analysis of flow and vortex dynamics in the near wake. The direct numerical simulations are performed at a Reynolds number of 100, the wave steepness of 0.025, and the non-dimensional wavelength of 5.6.

In an original Cartesian coordinate (x', y', z'), the geometric disturbance on the square-section cylinder is introduced in (x', z') plane, prescribed mathematically by $\xi(z') = -\frac{W}{2}\cos(2\pi z'/\lambda)$. The peak and valley of waviness are positions at $z' = 0, \lambda$ and $\lambda/2$, respectively, while the inflexion points are positions of $\xi(z') = 0$. The slope of waviness is $d\xi/dz'$. The mapping transformation[7] between the original system and new transformed coordinate system is introduced as, $x = x' - \xi(z')$, $y = y'$, $z = z'$, for the convenience in the generation of computational mesh. Then the velocity and the static pressure are transformed as: $u = u' - w'd\xi/dz'$, $v = v'$, $w = w'$ and $p = p'$. The dimensionless continuity and Navier-Stokes equations in terms of the transformed coordinates[5,7] will become

$$\nabla \cdot \boldsymbol{u} = 0, \tag{1a}$$

$$\frac{\partial \boldsymbol{u}}{\partial t} + \nabla \cdot (\boldsymbol{u}\boldsymbol{u}) = -\nabla p + \frac{1}{Re}\nabla^2 \boldsymbol{u} + \boldsymbol{A}, \tag{1b}$$

where lengths are scaled by the base height of the cylinder D and velocities by uniform inflow velocity U_∞, the Reynolds number is defined as $Re = U_\infty D/\nu$ in which ν is the kinematic viscosity of the fluid, and $\boldsymbol{A}$ is the extra term written as

$$A_x = -\left[\frac{d^2\xi}{dz^2}w^2 + \left(\frac{d\xi}{dz}\right)^2 \frac{\partial p}{\partial x} - \frac{d\xi}{dz}\frac{\partial p}{\partial z}\right]$$

*Supported by the National High-Tech Research and Development Program of China under Grant No 2006AA09Z350, and the Knowledge Innovation Program of Chinese Academy of Sciences under Grant No KJCX2-YW-L02.

**Email: llm@lnm.imech.ac.cn

$$+\frac{1}{Re}\left[\frac{\partial^2 u}{\partial z'^2}-\frac{\partial^2 u}{\partial z^2}+2\frac{d^2\xi}{dz^2}\frac{\partial w}{\partial z'}+\frac{d^3\xi}{dz^3}w\right], \quad (2a)$$

$$A_y=\frac{1}{Re}\left[\frac{\partial^2 v}{\partial z'^2}-\frac{\partial^2 v}{\partial z^2}\right], \quad (2b)$$

$$A_z=\frac{d\xi}{dz}\frac{\partial p}{\partial x}+\frac{1}{Re}\left[\frac{\partial^2 w}{\partial z'^2}-\underline{\frac{\partial^2 w}{\partial z^2}}\right], \quad (2c)$$

where the term with the underline is correctly pointed out, rather than $d^2\xi/dz^2$ used in Darekar and Sherwin. Then the wavy cylinder is straighten in computation.

With the assumption of the spanwise periodicity of the flow, the hybrid method combining Fourier spectral and finite difference is adopted with the multigrid solver used in the pressure Poisson equation. The second-order implicit scheme in time and the central difference scheme in space are applied. Boundary conditions for velocities in the (x, y) plane are employed: the uniform flow at inlet, the non-reflecting boundary condition at outlet, the free slip condition at vertical boundaries, and the non-slip condition on cylinder surfaces. The compatible normal gradient of pressure is imposed at all boundaries. The whole sizes of non-dimensional computational domain are $27 \times 18 \times 5.6$ $(x \times y \times z)$. The staggered grids in the (x, y) plane are 248×160 cells. The number of the Fourier mode is 18. The magnitude of convergent error in the continuity equation is about 10^{-3}. The numerical simulation for the flow past the non-wavy cylinder at $Re = 100$ has shown that the wake dynamics are described by the normal alternating Kármán vortex shedding. It should be noted that the phenomena for the wavy cylinder are described in the physical system (x', y', z'), while those for the non-wavy cylinder in the system (x, y, z) because of the computations carried out in the same system.

For the validation of computational codes, two-dimensional numerical experiments are made in the larger domain (50×48) with basic uniform grids of 0.25, 0.25 and 0.16 upstream, vertically and downstream, respectively, and 0.005 near the cylinder surface.[6] The Strouhal number St is 0.145, mean drag coefficient $\bar{C}_D$ 1.452 and RMS lift coefficient C'_L 0.179. Other scales of uniform grids, such as Δ_O of 0.1 and 0.2 downstream, are tested. For example, when Δ_O decreases to 0.1, $St = 0.145$, $\bar{C}_D = 1.452$, and $C'_L = 0.181$, while only C'_L decreases to 0.178 with Δ_O of 0.2. Other computations have also confirmed that the variation of grids is associated with the deviation of most hydrodynamic parameters within 5%. Therefore, the applied computational codes are stable and convergent.

Numerical results have shown that the introduction of disturbance does result in the original Kármán vortex shedding totally suppressed in the near wake and the flow being steady. The flow pattern of the suppression of vortex shedding is described by iso-surfaces of vorticity $(\omega'_x, \omega'_y, \omega'_z)$, pressure coefficient (C_p) and λ_2-definition $(\lambda_2 = -0.01)$,[8] as shown in Fig. 1. The vorticity is mainly concentrated in the near wake (see in Figs. 1(a) and 1(b)). Such pattern is like the two-finger hands stretching downstream illuminated by λ_2-definition, called the 'Chayote'-like vortex. Qualitatively, the vertical and streamwise components of vorticity near the cylinder surface and in the near wake, as well as on the rear surface, are alternately distributed with opposite signs and symmetric or antisymmetric about the wake center plane $(y' = 0)$, as shown in Fig. 1(a). However, the shear layers, described by the iso-surface of spanwise vorticity in Fig. 1(b), are elongated downstream without the vortex shedding. The wake is widened near the valley, indicating that the interaction between the upper and lower layers is delayed by the disturbance. Meanwhile, the pressure varied almost uniformly in $y' \in (-D/2, D/2)$ is different from that in the non-wavy cylinder in Fig. 4, implying the steady flow downstream.

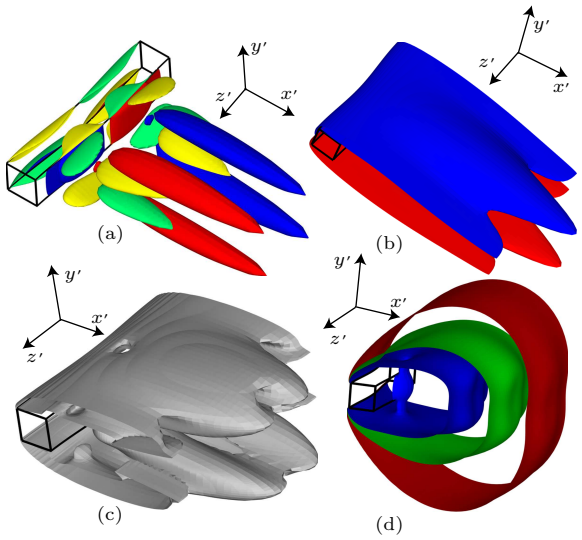

Fig. 1. Wake topology described by iso-surfaces of (a) (ω'_x, ω'_y) and (b) ω'_z, (c) λ_2 description[5] and (d) iso-surfaces of C_p. In (a), $\omega'_x = \pm 0.25$ (yellow/green) and $\omega'_y = \pm 0.5$ (red/blue). In (b), $\omega'_z = \pm 1.0$ (red/blue). In (d), $C_p = -0.1$ (red), -0.3 (green) and -0.5 (blue). The black framework indicates the wavy square cylinder.

An important feature, the vertical vorticity relatively stronger than the streamwise component, is presented not only on the rear surface but also in the near wake or shear layers. It can be explained by the following mechanism on the rear surface (denoted by the subscript $+x$), as suggestive of Ling and Lin,[5] as

$$\omega'_x/\omega'_z\big|_{+x} = d\xi/dz',$$
$$\omega'_y|_{+x} = -\left[1+\left(\frac{d\xi}{dz'}\right)^2\right]\frac{\partial w'}{\partial x'}\bigg|_{+x}. \quad (3)$$

The streamwise vorticity is directly resulted from the effect of disturbance on the spanwise component, while the vertical vorticity is only related with the induced spanwise flow. Quantitatively, $\omega'_x|_{+x}$ is linearly varied with the wavy steepness and limited in

the magnitude of W/λ, while $\omega'_y|_{+x}$ is non-linearly amplified by disturbance.[6] As shown in Fig. 2, the ratio $|\omega'_{y\max}/\omega'_{x\max}|$ is nearly up to 40, indicating the appearance of spanwise flow being stronger, especially at the wake center plane (see Fig. 3(a)).

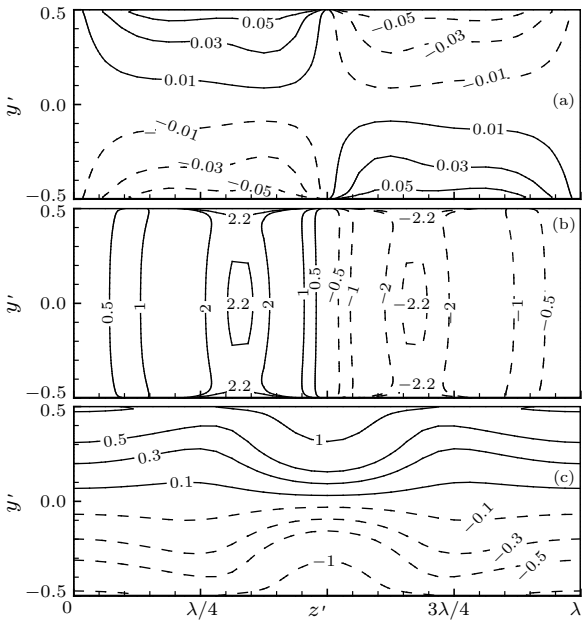

Fig. 2. Distributions of (a) streamwise, (b) vertical and (c) spanwise components of vorticity on the rear surface, where solid and dashed lines denote the positive and negative values.

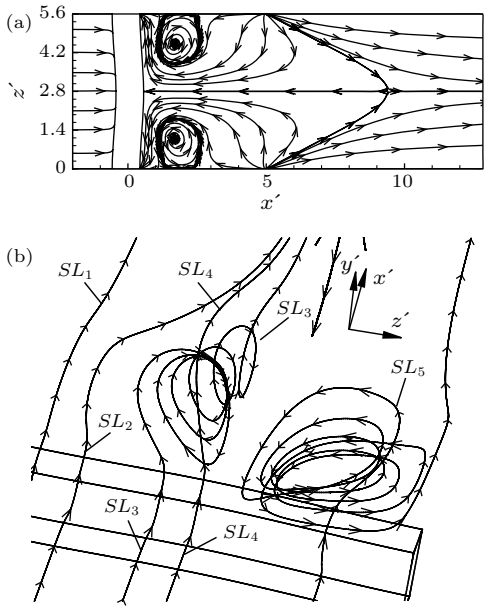

Fig. 3. Flow pattern described by typical streamlines in (a) the wake center plane and (b) the near wake, where $SL_n(n = 1 \sim 5)$ denotes streamlines starting from different positions.

Then the streamlines are influenced by the above specific distribution of streamwise and vertical components of vorticity. Without the interference of geometric disturbance at $Re = 100$, the streamlines in (x, y) plane are only encircle the Kármán vortex alternately shedding, leading to the wavy terrain (see Fig. 4). However, in the 'Chayote'-like vortex, as shown in Fig. 5, ω'_x is mainly distributed near the wake center plane, while ω'_y is distributed in the wider region in the near wake. Correspondingly, the streamlines turn to the spanwise direction, encircle around such concentrated vertical vorticity and further form the recirculating cells in the near wake, as shown in Fig. 3(a) and like SL_3 and SL_5 in Fig. 3(b). The recirculating cells extend along the y' direction until the upper and lower shear layers. Near the peak and valley, the streamlines, like SL_1, SL_2 and SL_4 in Fig. 3(b), simply go around the fully developed recirculating cells.

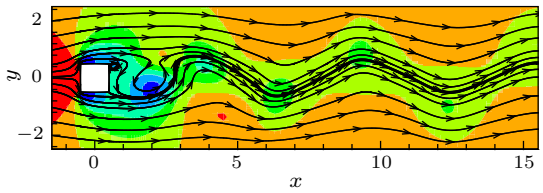

Fig. 4. Kármán vortex shedding described by instantaneous streamlines and contours of pressure coefficients (from −0.5(blue) to 0(red)) in the straight cylinder at $Re = 100$.

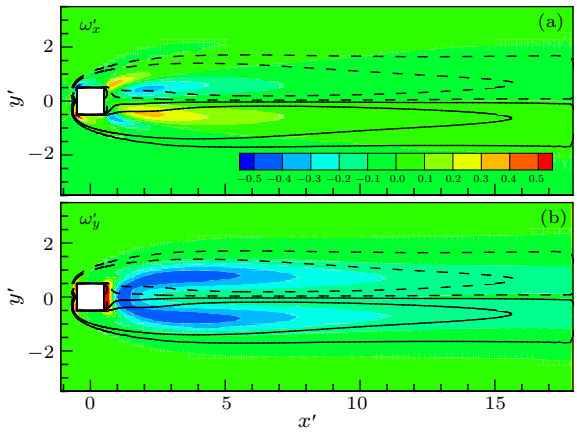

Fig. 5. Distributions of (a) ω'_x and (b) ω'_y at the inflexion point $z' = \lambda/4$, where the background contours are ω'_z of ± 0.1 and ± 0.5 with solid and dashed lines indicating positive and negative values.

On the other hand, such distribution of vertical vorticity reinforces the flow in the spanwise direction downstream and relatively weakens that in the vertical direction (see the comparison between Fig. 6(a) and Fig. 6(b)). The alternating distribution of $\pm|v|$ in the Kármán vortex is disappeared. Therefore, the shear layers could not roll up into the vortex rolls, but further stretch into the far wake. In other words, the geometric disturbance enhances the stability of the shear layers without shedding. In addition, in the near wake, the series of closed vortex lines is regularly formed downstream due to the vertical vorticity, as shown in Fig. 7. These vortex lines are initially generated on the rear and lateral surfaces of cylinder.[6] This further confirms the way of the linkage of the

upper and lower shear layers by the vertical vorticity, as one of possible flow patterns in the study of vortex shedding suppression.

Therefore, the vital role played in the complete suppression of Kármán vortex shedding or the formation of 'Chayote'-like vortex is the vertical vorticity, rather than the streamwise component.[4] In Fig. 5(a), the streamwise vorticity near the leading edge and the rear surface, and in the near wake changes its sign twice, indicating the disturbed shear layers qualitatively different downstream if the effect of streamwise vorticity is dominant. However, the upper and lower shear layers are always kept away from each other at the valley.

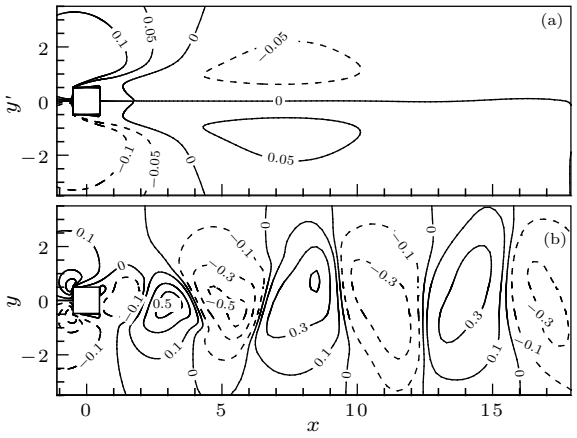

Fig. 6. Contours of (a) the vertical component of velocity in the case of vortex suppression at $z' = \lambda/4$, and in comparison with (b) that in the non-wavy cylinder.

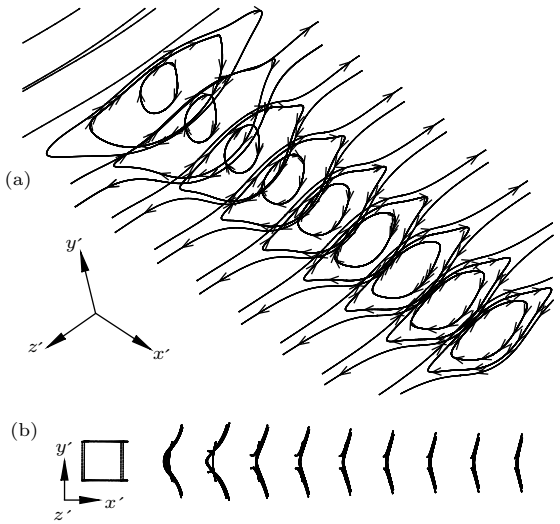

Fig. 7. Wake dynamics described by the spatial evolution of vortex filaments in (a) side view and (b) (x', y')-plane view.

Finally, from profiles of streamwise velocity in the wake in Fig. 8, the spanwise waviness in wake profiles appears first near the rear surface, reaches up to the maximum in the near wake and decays in the far wake. The wake profile at $x = 2.783$, remarkably different from the classical wake profile in the non-wavy cylinder, is very similar to that used in the study of the wake-type flow.[9] The complete suppression of vortex shedding is also observed by introducing the disturbance on the upstream velocity profile. The vertical vorticity as a unique additional vorticity is directly resulted from such disturbance. The natural instability of shear layers in the wake-type inflow becomes stable. The shear layers stretch into the far wake too. This further confirms the important role of vertical vorticity in the mechanism of suppression.

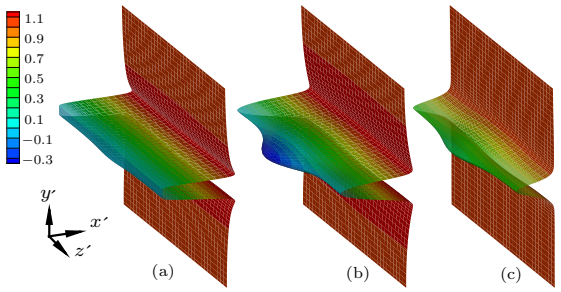

Fig. 8. Wake profiles described by u' at different relative positions $x(= x' - \xi(z'))$ of (a) 0.615, (b) 2.783 and (c) 12.5.

In summary, the present simulations, especially the characteristics of vorticity on the rear surface and in the near wake, have shown that the effect of the vertical vorticity is dominant on the formation of the 'Chayote'-like vortex, while the streamwise component is nearly negligible, which is inconsistent with the result suggested by Darekar and Sherwin. Based on the present study, a new mechanism responsible for the suppression of Kármán vortex is proposed as follows. The disturbance on the rear surface leads to the appearance of spanwise flow near the base of the cylinder. The vertical vorticity is also generated on the rear surface with the magnitude nonlinearly amplified greatly, and convected into the near wake. Therefore, the traditional wake flow in the near-base region mainly turns to the spanwise direction predominantly and further recirculates, leading to the formation of the pair of recirculating cells. The upper and lower shear layers are apart from each other due to such cells extending along the vertical direction. Then these layers stretch downstream without the formation of vortex rolls. The near wake becomes stable.

References

[1] Roshko A 1955 *J. Aeronaut. Sci.* **22** 124
[2] Bearman P W 1965 *J. Fluid Mech.* **21** 241
[3] Bearman P W and Owen J C 1998 *J. Fluids Struct.* **12** 123
[4] Darekar R M and Sherwin S J 2001 *J. Fluid Mech.* **426** 263
[5] Ling G C and Lin L M 2008 *Acta Mech. Sin.* **24** 101
[6] Lin L M 2007 *PhD thesis* (Beijing: Institute of Mechanics, Chinese Academy of Sciences) (in Chinese)
[7] Newman D J and Karniadakis G E 1997 *J. Fluid Mech.* **344** 95
[8] Jeong J and Hussain F 1995 *J. Fluid Mech.* **285** 69
[9] Ling G C and Zhao H L 2009 *Phys. Fluids* **21** 073604